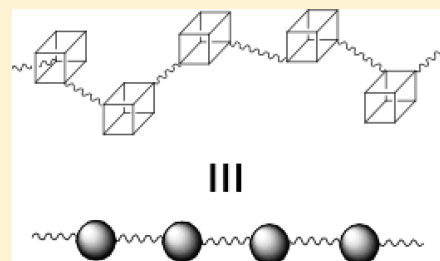


Beads on a Chain (BOC) Polymers Formed from the Reaction of $\text{NH}_2\text{PhSiO}_{1.5}]_x[\text{PhSiO}_{1.5}]_{10-x}$ and $[\text{NH}_2\text{PhSiO}_{1.5}]_x[\text{PhSiO}_{1.5}]_{12-x}$ Mixtures ($x = 2-4$) with the Diglycidyl Ether of Bisphenol A

Jae Hwan Jung[†] and Richard M. Laine^{*,†,‡}

[†]Macromolecular Science and Engineering and [‡]Materials Science and Engineering, University of Michigan, Ann Arbor, Michigan 48109-2136, United States

ABSTRACT: We recently reported that catalytic amounts of F^- cause rapid rearrangement of silsesquioxane (SQ) T_8 cages in THF at room temperature. These rearrangements lead primarily to the T_{10} and T_{12} cages as long as the F^- is trapped for example using CaCl_2 to form insoluble CaF_2 in situ. In this report, we use this approach to make di- and triaminophenyl, phenyl silsesquioxane T_{10} and T_{12} mixtures: $(\text{NH}_2\text{Ph})_{2x}\text{Ph}_{10/12-x}(\text{SiO}_{1.5})_{10/12}$. Thereafter, we isolate the fraction that consists primarily of $x = 2-3$ via column chromatography. We then explore the reaction of this fraction (fraction 3) with the diglycidyl ether of bisphenol A (DGEBA) to form a soluble epoxy resin wherein the cage SQs are contained in the chain backbone. We call these products beads on a chain (BoC) polymers. The use of 1:1 mole ratios of [epoxide]: $[\text{NH}_2\text{Ph}]$ of DGEBA and $(\text{NH}_2\text{Ph})_{2x}\text{Ph}_{10/12-x}(\text{SiO}_{1.5})_{10/12}$ leads to insoluble products. However, the reaction of 0.8:1 mole ratio of [epoxide]: $[\text{NH}_2\text{Ph}]$ provides a soluble but bimodal distribution of products (after 24 h reaction at 90 °C in THF). The low MW component is much more soluble in THF than the higher MW component, allowing simple separation. The low MW polymer has a M_n of 6000 Da with a PDI of 1.6. The higher MW material has an M_n of 21 000 000 Da with a PDI of 21. Both components offer similar ceramic yields (to SiO_2) of $32 \pm 1\%$, indicating that the relative contents of cages are identical. They also exhibit very similar FTIR spectra, suggesting that they are the same material. Two explanations are possible for the bimodal size distribution. One is that the positioning of the NH_2 groups on the cage leads to cyclic trimers given that the average monomer unit will mass $\approx 1700-1900$ Da, which represents the low MW fraction. Alternately and more likely, the higher molecular weight component consists of di- and triamino functionalities such that in the growing chain, once the first two amine groups on the cage react, the third group is likely sterically protected. Thus, only late in the reaction will the quantities of the third group exceed those of the diamino components, allowing a slow tertiary functionalization and likely some degree of cross-linking (or internal cyclization) to occur. That this happens is suggested by the much poorer solubility of the higher MW materials as well as the very large PDI. These studies serve as a model for other possible studies targeting BoC polymers.



INTRODUCTION

There is recent, intense interest in the use of silsesquioxane (SQ) cages as nanobuilding blocks for the synthesis and processing of nanocomposite materials and as sites for attaching multiple types of functionalities for diverse applications as witnessed by the publication of 17 reviews over the past 30 years, with the majority published in the past 10 years.¹⁻¹⁷ Despite the now thousands of articles and patents concerning SQs, the number of papers that describe the synthesis and properties of SQs as part of a polymer backbone is limited to just a few studies.¹⁸⁻²⁴

Some examples of difunctional silsesquioxane monomers and what we propose to call “beads on a chain” (BoC) polymers are those shown in Schemes 1 and 2.²⁴

In part, this problem arises because until now it has been difficult to synthesize SQs with just two or three functional groups on the cage that would permit their copolymerization with other monomer units. Most SQs or POSS compounds currently described in the literature either have only 1 or 8, 16, or

even 24 functional groups or functional group equivalents attached to the cage vertices.^{1-17,25-27} However, the opportunity to synthesize di- and trifunctional SQs, especially in T_{10} and T_{12} cages and BoC polymers, therefrom now exists.²⁸

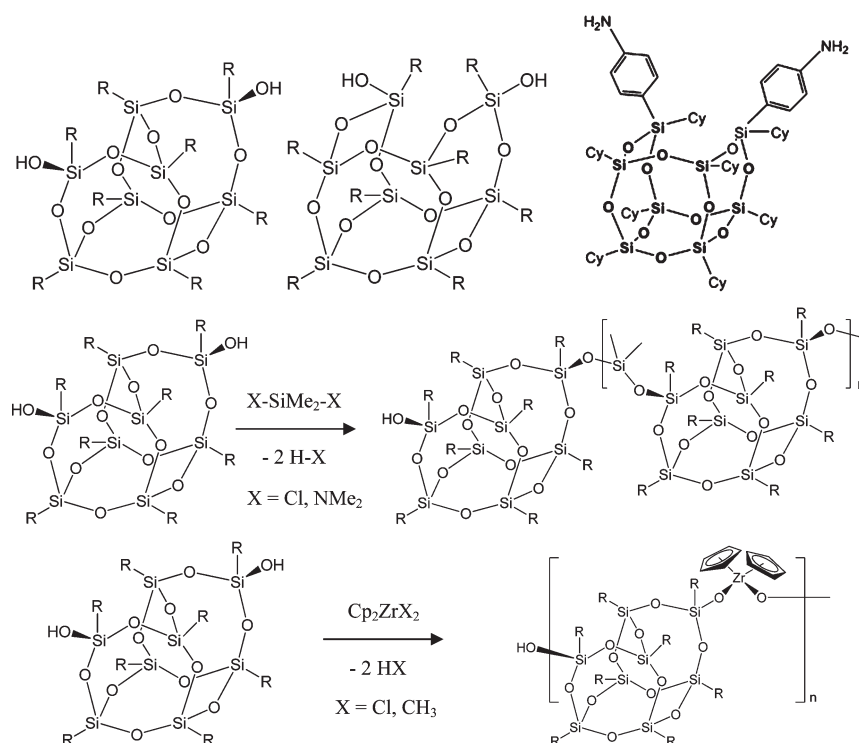
We recently described using F^- in the form of tBu_4NF to catalyze the rapid equilibration of functional groups between two types of polysilsesquioxanes or from SQ resins in THF at room temperature to form T_{10} and T_{12} mixed functional SQs as suggested in Scheme 3.²⁸⁻³⁰ We report here an extension of this method to the synthesis of di- and triarylamino cages targeting the synthesis of BoC polymers that represent new classes of curing agents for epoxy resins and possible comonomers for the synthesis of polyamides and polyimides. One key objective is to take advantage of the robust nature of SQs to develop families of high-temperature stable, soluble, and processable BoC polymer systems.

Received: May 11, 2011

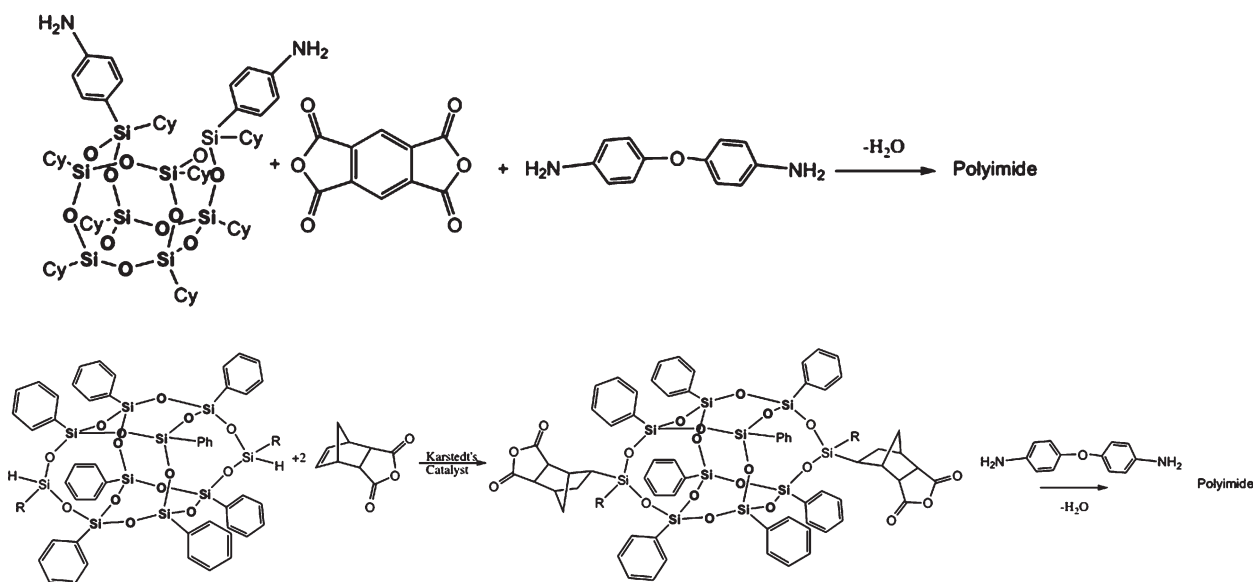
Revised: August 3, 2011

Published: September 02, 2011

Scheme 1. Examples of Difunctional SQs and Examples of Polymerization via Si–OH Bonds of “Beads on a Chain” (BoC) Polymers (R = Cy = Cyclohexyl)²⁴



Scheme 2. Polymerization of Difunctional SQs to BoC Polyimides^{18–23}

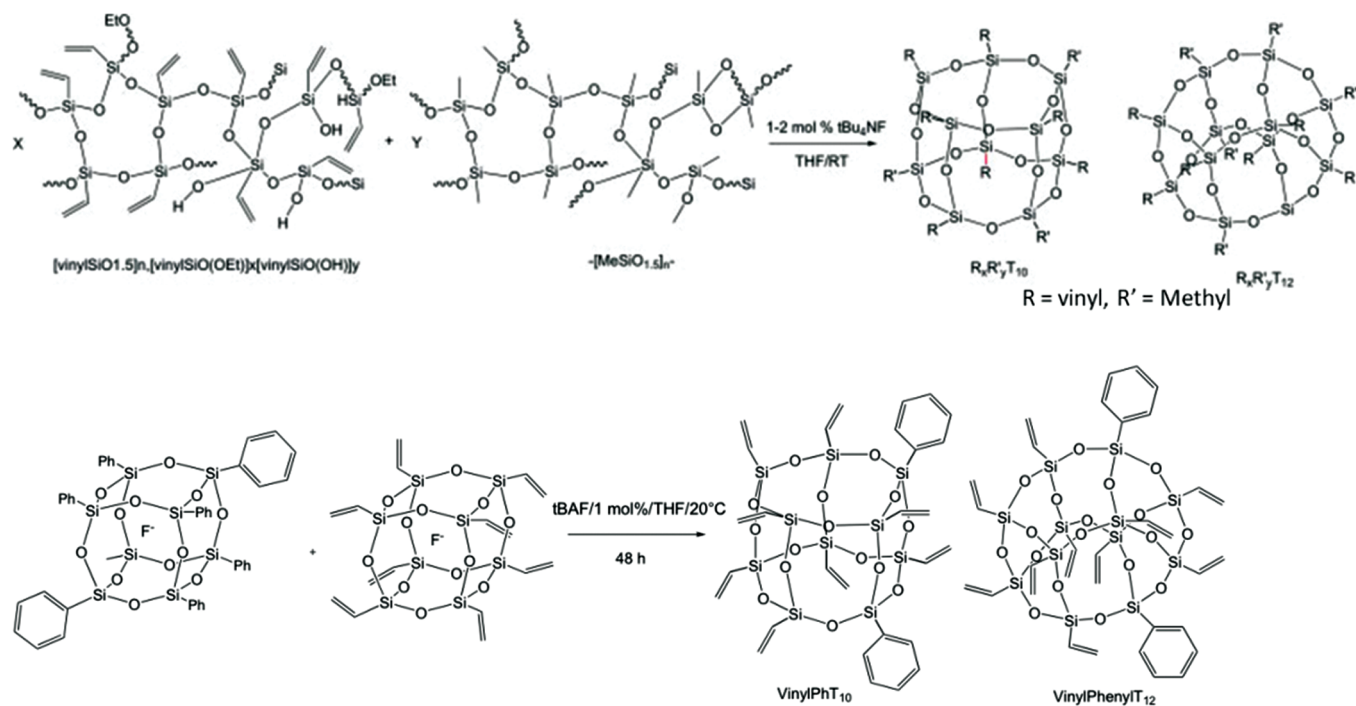


EXPERIMENTAL SECTION

Materials. Octaphenylsilsesquioxane [(C₆H₅SiO_{1.5})₈, OPS] and octaaminophenylsilsesquioxane [(NH₂C₆H₄SiO_{1.5})₈, OAPS] were prepared using literature methods or received as gifts from Mayaterials Inc.¹⁶ Diglycidyl ether of bisphenol A (DGEBA) (DER 331, MW 372) was purchased from Dow Chemical Corp. (Midland, MI). All other chemicals were purchased from Aldrich or Fisher and used as received.

All manipulations were performed under nitrogen unless otherwise stated.

Synthetic Methods. *Synthesis of [NH₂PhSiO_{1.5}]_x[PhSiO_{1.5}]_{10/12-x}.* To an oven-dried, 100 mL Schlenk flask under N₂, equipped with a magnetic bar was added 0.27 g (0.24 mmol) of OAPS and 0.73 g (0.47 mmol) of OPS. THF (20 mL) was added by syringe followed by 0.036 mL (0.036 mmol, 5.0 mol % OPS and OAPS) of 95% tetra-*n*-butylammonium fluoride (TBAF) solution (1.0 M in THF). The mixture was stirred at

Scheme 3. F^- -Catalyzed Formation of T_{10} and T_{12} SQs from Polymeric SQ Resins or T_8 CagesTable 1. MALDI-TOF Data for 3:1 OPS:OAPS Reaction with TBAF^a

most common isotope	found (Da)	calcd (Da)	relative peak intensities (%)
$(C_6H_5)_8(SiO_{1.5})_8 (+ Ag^+)$	1140.8	1141.4	5
$(NH_2C_6H_4)_1(C_6H_5)_7(SiO_{1.5})_8 (+ Ag^+)$	1155.9	1156.5	17
$(NH_2C_6H_4)_2(C_6H_5)_6(SiO_{1.5})_8 (+ Ag^+)$	1170.8	1171.5	18
$(NH_2C_6H_4)_3(C_6H_5)_5(SiO_{1.5})_8 (+ Ag^+)$	1185.9	1186.5	12
$(C_6H_5)_{10}(SiO_{1.5})_{10}$	1292.7	1291.8	7
$(NH_2C_6H_4)_1(C_6H_5)_9(SiO_{1.5})_{10}$	1308.7	1307.8	21
$(NH_2C_6H_4)_2(C_6H_5)_8(SiO_{1.5})_{10}$	1323.7	1323.8	28
$(NH_2C_6H_4)_3(C_6H_5)_7(SiO_{1.5})_{10}$	1338.7	1339.9	18
$(C_6H_5)_{10}(SiO_{1.5})_{10} (+ Ag^+)$	1398.6	1399.8	25
$(NH_2C_6H_4)_1(C_6H_5)_9(SiO_{1.5})_9 (+ Ag^+)$	1413.6	1414.8	81
$(NH_2C_6H_4)_2(C_6H_5)_8(SiO_{1.5})_8 (+ Ag^+)$	1428.6	1429.8	100
$(NH_2C_6H_4)_3(C_6H_5)_8(SiO_{1.5})_7 (+ Ag^+)$	1443.6	1444.8	69
$(C_6H_5)_{12}(SiO_{1.5})_{12}$	1551.5	1551.2	4
$(NH_2C_6H_4)_1(C_6H_5)_{11}(SiO_{1.5})_{12}$	1566.5	1566.2	8
$(NH_2C_6H_4)_2(C_6H_5)_{10}(SiO_{1.5})_{12}$	1581.5	1582.2	13
$(NH_2C_6H_4)_3(C_6H_5)_9(SiO_{1.5})_{12}$	1598.4	1598.2	8
$(C_6H_5)_{12}(SiO_{1.5})_{12} (+ Ag^+)$	1567.4	1568.2	3
$(NH_2C_6H_4)_1(C_6H_5)_{11}(SiO_{1.5})_{12} (+ Ag^+)$	1672.3	1673.2	11
$(NH_2C_6H_4)_2(C_6H_5)_{10}(SiO_{1.5})_{12} (+ Ag^+)$	1687.4	1688.2	12
$(NH_2C_6H_4)_3(C_6H_5)_9(SiO_{1.5})_{12} (+ Ag^+)$	1702.4	1703.2	8

^a Error in reported intensities is $\pm 5\%$.

room temperature for 72 h, and any unreacted OPS was removed by filtration in N_2 . Calcium chloride powder ($CaCl_2$, 0.6 g) was added to the filtrate, and the mixture stirred at room temperature for 2 h. After filtering again, solvent was dried *in vacuo* providing 0.85 g of a dark brown solid equal to an 85% yield. This solid was purified by column chromatography on silica. The product was eluted using an 8:2 ratio of methylene

chloride:hexane followed by THF (column yield: 30%). Characterization data: 1H NMR (400 MHz, $DMSO-d_6$): δ 4.5–5.5 (br, $-NH_2$), 6.5–8.0 (br, Ar–H). IR: ν_{N-H} (3380), ν_{C-H} (3230–2840), $\nu_{C=C}$ (Ar ring, 1594), $\nu_{C=C}$ (Ar ring, 1430), $\nu_{Si-O-Si}$ (1230–960), ν_{Si-C} (740) cm^{-1} . MALDI-TOF: m/z = 1171 $[AgSi_8O_{12}(C_6H_5)_6(NH_2C_6H_4)_2]$, 1324 $[Si_{10}O_{15}(C_6H_5)_8(NH_2C_6H_4)_2]$, 1340 $[Si_{10}O_{15}(C_6H_5)_7(NH_2C_6H_4)_3]$,

Table 2. MALDI-TOF Peak Intensities for Several Ratio of OPS:OAPS Reaction with TBAF^a

most common isotope	2.5:1	3:1	4:1
(C ₆ H ₅) ₈ (SiO _{1.5}) ₈ (+ Ag ⁺)	4	5	20
(NH ₂ C ₆ H ₄) ₁ (C ₆ H ₅) ₇ (SiO _{1.5}) ₈ (+ Ag ⁺)	16	17	17
(NH ₂ C ₆ H ₄) ₂ (C ₆ H ₅) ₆ (SiO _{1.5}) ₈ (+ Ag ⁺)	22	18	13
(NH ₂ C ₆ H ₄) ₃ (C ₆ H ₅) ₅ (SiO _{1.5}) ₈ (+ Ag ⁺)	14	12	5
(C ₆ H ₅) ₁₀ (SiO _{1.5}) ₁₀	9	7	18
(NH ₂ C ₆ H ₄) ₁ (C ₆ H ₅) ₉ (SiO _{1.5}) ₁₀	31	21	19
(NH ₂ C ₆ H ₄) ₂ (C ₆ H ₅) ₈ (SiO _{1.5}) ₁₀	50	28	40
(NH ₂ C ₆ H ₄) ₃ (C ₆ H ₅) ₇ (SiO _{1.5}) ₁₀	40	18	15
(C ₆ H ₅) ₁₀ (SiO _{1.5}) ₁₀ (+ Ag ⁺)	17	25	70
(NH ₂ C ₆ H ₄) ₁ (C ₆ H ₅) ₉ (SiO _{1.5}) ₁₀ (+ Ag ⁺)	69	81	100
(NH ₂ C ₆ H ₄) ₂ (C ₆ H ₅) ₈ (SiO _{1.5}) ₁₀ (+ Ag ⁺)	100	100	91
(NH ₂ C ₆ H ₄) ₃ (C ₆ H ₅) ₇ (SiO _{1.5}) ₁₀ (+ Ag ⁺)	87	69	42
(C ₆ H ₅) ₁₂ (SiO _{1.5}) ₁₂	11	4	5
(NH ₂ C ₆ H ₄) ₁ (C ₆ H ₅) ₁₁ (SiO _{1.5}) ₁₂	18	8	20
(NH ₂ C ₆ H ₄) ₂ (C ₆ H ₅) ₁₀ (SiO _{1.5}) ₁₂	17	13	16
(NH ₂ C ₆ H ₄) ₃ (C ₆ H ₅) ₉ (SiO _{1.5}) ₁₂	7	8	3
(C ₆ H ₅) ₁₂ (SiO _{1.5}) ₁₂ (+ Ag ⁺)		3	2
(NH ₂ C ₆ H ₄) ₁ (C ₆ H ₅) ₁₁ (SiO _{1.5}) ₁₂ (+ Ag ⁺)	7	11	7
(NH ₂ C ₆ H ₄) ₂ (C ₆ H ₅) ₁₀ (SiO _{1.5}) ₁₂ (+ Ag ⁺)	11	12	7
(NH ₂ C ₆ H ₄) ₃ (C ₆ H ₅) ₉ (SiO _{1.5}) ₁₂ (+ Ag ⁺)	12	8	3

^a Error in reported intensities is $\pm 5\%$.**Table 3. MALDI-TOF Data (Ag⁺ Adduct) for Fraction 1^a**

most common isotope	found (Da)	calcd (Da)	relative peak intensity (%)
(C ₆ H ₅) ₈ (SiO _{1.5}) ₈	1141.0	1141.4	24
(C ₆ H ₅) ₁₀ (SiO _{1.5}) ₁₀	1399.1	1399.8	100
(C ₆ H ₅) ₁₂ (SiO _{1.5}) ₁₂	1657.6	1658.2	4

^a Error in reported intensities is $\pm 5\%$.**Table 4. MALDI-TOF Data for Fraction 2^a**

most common isotope	found (Da)	calcd (Da)	relative peak intensity (%)
(NH ₂ C ₆ H ₄) ₁ (C ₆ H ₅) ₇ (SiO _{1.5}) ₈ (+ Ag ⁺)	1156.9	1156.5	11
(NH ₂ C ₆ H ₄) ₁ (C ₆ H ₅) ₉ (SiO _{1.5}) ₁₀	1308.0	1307.8	45
(NH ₂ C ₆ H ₄) ₂ (C ₆ H ₅) ₈ (SiO _{1.5}) ₁₀	1323.1	1323.8	17
(NH ₂ C ₆ H ₄) ₁ (C ₆ H ₅) ₉ (SiO _{1.5}) ₁₀ (+ Ag ⁺)	1414.9	1414.8	100
(NH ₂ C ₆ H ₄) ₁ (C ₆ H ₅) ₁₁ (SiO _{1.5}) ₁₂ (+ Ag ⁺)	1672.9	1673.2	7

^a Error in reported intensities is $\pm 5\%$.

1430 [AgSi₁₀O₁₅(C₆H₅)₈(NH₂C₆H₄)₂], 1444 [AgSi₁₀O₁₅(C₆H₅)₇(NH₂C₆H₄)₃], 1583 [Si₁₂O₁₈(C₆H₅)₁₀(NH₂C₆H₄)₂], 1599 [Si₁₂O₁₈(C₆H₅)₉(NH₂C₆H₄)₃], 1171 [AgSi₁₂O₁₈(C₆H₅)₁₀(NH₂C₆H₄)₂] amu (see Table 4). GPC (found): *M_n* 1250; *M_w* 1290; PDI 1.04. TGA (air, 1000 °C): found 45.1%; *T_{d5%}* = 450 °C (see also Tables 1–7).

Polymerization of [(NH₂Ph)₂xPh_{10/12-x}(SiO_{1.5})_{10/12}] with DGEBA. To a dry 25 mL round-bottom flask equipped with magnetic stirrer were added (NH₂Ph)₂xPh_{8/10-x}(SiO_{1.5})_{10/12} (1.0 g, 2.0 mmol of

Table 5. MALDI-TOF Data for Fraction 3^a

most common isotope	found (Da)	calcd (Da)	relative peak intensity (%)
(NH ₂ C ₆ H ₄) ₂ (C ₆ H ₅) ₆ (SiO _{1.5}) ₈ (+ Ag ⁺)	1170.8	1171.5	13
(NH ₂ C ₆ H ₄) ₂ (C ₆ H ₅) ₈ (SiO _{1.5}) ₁₀	1323.6	1323.8	38
(NH ₂ C ₆ H ₄) ₃ (C ₆ H ₅) ₇ (SiO _{1.5}) ₁₀	1339.6	1339.9	9
(NH ₂ C ₆ H ₄) ₂ (C ₆ H ₅) ₈ (SiO _{1.5}) ₁₀ (+ Ag ⁺)	1429.5	1429.8	100
(NH ₂ C ₆ H ₄) ₃ (C ₆ H ₅) ₇ (SiO _{1.5}) ₁₀ (+ Ag ⁺)	1443.6	1444.8	40
(NH ₂ C ₆ H ₄) ₂ (C ₆ H ₅) ₁₀ (SiO _{1.5}) ₁₂	1582.5	1582.2	22
(NH ₂ C ₆ H ₄) ₃ (C ₆ H ₅) ₉ (SiO _{1.5}) ₁₂	1598.5	1598.2	29
(NH ₂ C ₆ H ₄) ₂ (C ₆ H ₅) ₁₀ (SiO _{1.5}) ₁₂ (+ Ag ⁺)	1687.4	1688.2	9

^a Error in reported intensities is $\pm 5\%$.**Table 6. Decomposition Temperatures (*T_{d5%}*) and Ceramic Yields for [(NH₂Ph)₂xPh_{10/12-x}(SiO_{1.5})_{10/12}] (Fraction 3) and Starting Materials (Air/10 °C/min to 1000 °C)^a**

compound	<i>T_{d5%}</i> (°C)	ceramic yield (%)	theor ceramic yield (%)
OPS	465	47.1	46.5
OAPS	360	42.0	41.7
fraction 3	450	45.2	

^a Theoretical ceramic yields for compounds detected by MALDI are given for reference.**Table 7. GPC Determined Molecular Weights and Polydispersities of Figure 7 Components**

	<i>t_R</i> (min)	<i>M_n</i>	<i>M_w</i>	PDI
OPS	33.3	940	945	1.01
OAPS	31.9	1450	1490	1.03
3:1 OPS:OAPS reaction product	32.3	1330	1410	1.06
fraction 3	32.5	1250	1290	1.04

Table 8. GPC Determined Molecular Weights and Polydispersities of Figure 9 Components

	<i>M_n</i>	<i>M_w</i>	PDI
BoC polymer	9000	74000000	8000
low <i>M_w</i> polymer	6000	10000	1.6
high <i>M_w</i> polymer	12600000	270000000	21

NH₂PH) and DGEBA (0.30 g, 0.81 mmol, 1.6 mmol of epoxy group). The flask was evacuated and flushed three times with N₂. 1,4-Dioxane (10 mL) was added via syringe. The reaction mixture was stirred at 90 °C for 24 h and monitored by GPC. Thereafter, the reaction mixture was precipitated into 150 mL of MeOH. The precipitated products were collected and dried *in vacuo* to give a brown powder (0.95 g, 73%). The product was further purified by selective dissolution in THF. Thus, 0.5 g of product was added to 10 mL of THF and stirred 2 h at room temperature. The solution was filtered and filtrate was precipitated in 100 mL of methanol (low molecular weight polymer, 0.21 g, 40%). The insoluble polymer was collected and 10 mL of THF was again added. This solution was sonicated for 6 h at 60 °C and then filtered, and the

filtrate precipitated in 100 mL of methanol (high molecular weight polymer, 0.15 g, 30%). Note that to avoid formation of highly cross-linked products only 80 mol % epoxy is added. Characterization data: ^1H NMR (400 MHz, $\text{DMSO}-d_6$): δ 1.2 (br, $-\text{CH}_3$), 3.5–4.3 (br, $\text{ArCH}_2\text{CH}_2\text{CHOHCH}_2$), 4.7–5.6 (br, $-\text{NH}$), 6.0–7.9 (br, $\text{Ar}-\text{H}$). IR: $\nu_{\text{O}-\text{H}}$ (3500), $\nu_{\text{C}-\text{H}}$ (3100–2800), $\nu_{\text{C}=\text{C}}$ (Ar ring, 1595), $\nu_{\text{C}-\text{O}}$ (1250), $\nu_{\text{Si}-\text{O}-\text{Si}}$ (1230–960), $\nu_{\text{Si}-\text{C}}$ (740) cm^{-1} . GPC (found): M_n 9000; M_w 74 000 000; PDI 8000 (see Tables 8 and 9). TGA (air, 1000 $^\circ\text{C}$): found 33.0%; $T_{d5\%} = 280$ $^\circ\text{C}$ (see Tables 8 and 9).

Analytical. NMR Analyses. All ^1H were performed in DMSO and recorded on a Varian INOVA 400 spectrometer. ^1H NMR spectra were collected at 400 MHz using a 6000 Hz spectral width, a relaxation delay of 3.5 s, a pulse width of 38°, 30K data points, and TMS (0.00 ppm) as an internal reference.

Matrix-Assisted Laser Desorption/Time-of-Flight Spectrometry. MALDI-ToF was done on a Micromass ToFSpec-2E equipped with a 337 nm nitrogen laser in positive-ion reflectron mode using poly(ethylene glycol) as calibration standard, dithranol as matrix, and AgNO_3 as ion source. Sample was prepared by mixing solution of 5 parts matrix (10 mg/mL in THF), 5 parts sample (1 mg/mL in THF), and 1 part of AgNO_3 (2.5 mg/mL in water) and blotting the mixture on the target plate.

Fourier-Transform Infrared Spectroscopy (FTIR). Diffuse reflectance Fourier transform (DRIFT) spectra were recorded on a Nicolet 6700 Series FTIR spectrometer (Thermo Fisher Scientific, Inc., Madison, WI). Optical grade, random cuttings of KBr (International Crystal Laboratories, Garfield, NJ) were ground, with 1.0 wt % of the sample to be analyzed. For DRIFT analysis, samples were packed firmly and leveled off at the upper edge to provide a smooth surface. The FTIR sample chamber was flushed continuously with N_2 prior to data acquisition in the range 4000–400 cm^{-1} .

Gel Permeation Chromatography. All GPC analyses were done on a Waters 440 system equipped with Waters Styragel columns (7.8×300 , HT 0.5, 2, 3, 4) with RI detection using Optilab DSP interferometric refractometer and THF as solvent. The system was calibrated using polystyrene standards and toluene as reference. Analyses were performed using PL Caliber 7.04 software (Polymer Laboratories, Shropshire, UK).

Table 9. Decomposition Temperatures ($T_{d5\%}$, $T_{d50\%}$) and Ceramic Yields of Synthesized Polymers and Starting Materials for Comparison (Air, 10 $^\circ\text{C}/\text{min}$ to 1000 $^\circ\text{C}$)

compound	$T_{d5\%}$ ($^\circ\text{C}$)	$T_{d50\%}$ ($^\circ\text{C}$)	ceramic yield (%)	theor ceramic yield (%)
DGEBA	295	370	0.0	
fraction 3	450	670	45.2	
BoC polymer	300	595	31.6	34.7
high M_w part	320	645	31.0	
low M_w part	330	635	33.2	

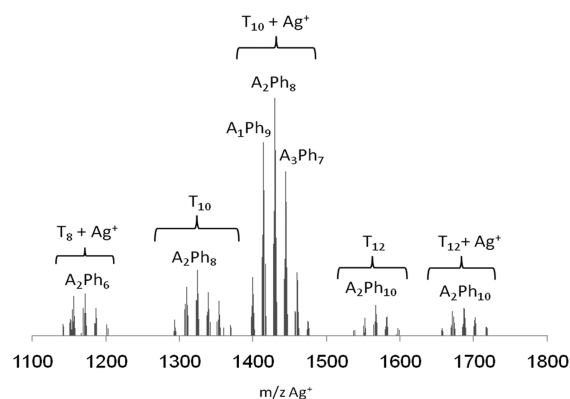


Figure 1. MALDI-TOF spectrum of 3:1 OPS:OAPS reaction with TBAF (RT/72 h).

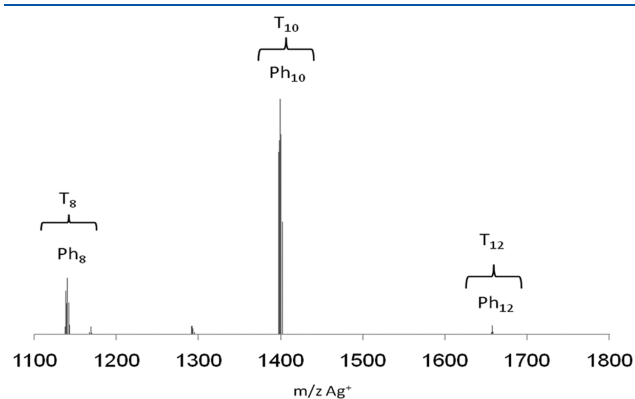


Figure 2. MALDI-TOF of fraction 1.

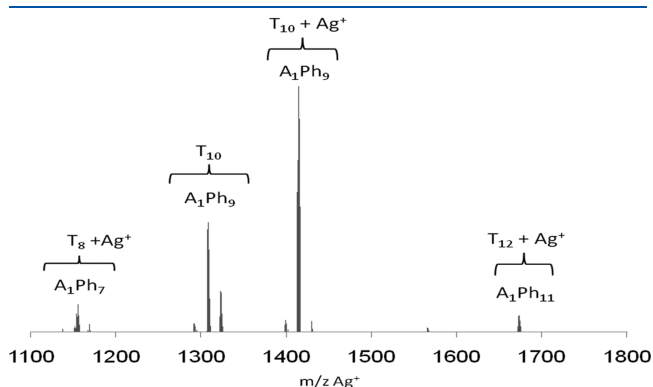
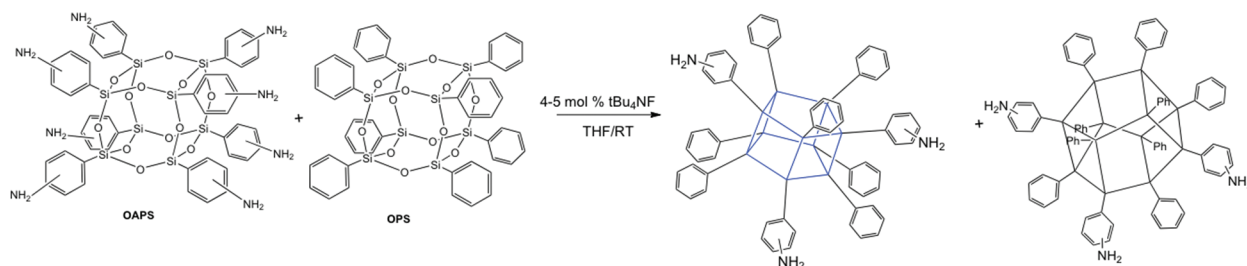


Figure 3. MALDI-TOF of fraction 2.

Scheme 4. F^- -Catalyzed Formation of $[(\text{NH}_2\text{Ph})_{2x}\text{Ph}_{10/12-x}(\text{SiO}_{1.5})_{10/12}]$ from OAPS and OPS



Thermal Gravimetric Analyses (TGA). Thermal stabilities of materials under N₂ or air were examined using a 2960 simultaneous DTA-TGA (TA Instruments, Inc., New Castle, DE). Samples (5–10 mg) were loaded in alumina pans and ramped to 1000 °C while heating at 10 °C/min. The N₂ or air flow at 60 mL/min.

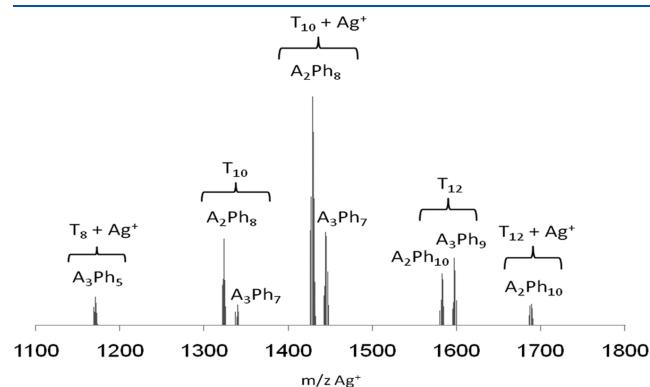


Figure 4. MALDI-TOF for fraction 3.

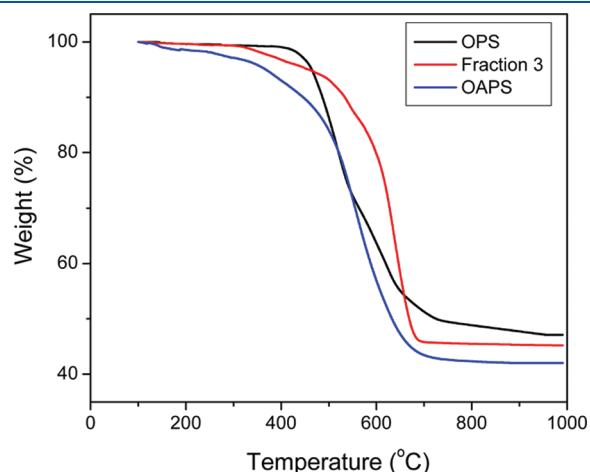


Figure 5. TGA of [(NH₂Ph)_{2x}Ph_{10/12-x}(SiO_{1.5})_{10/12}] (fraction 3) and OPS, OAPS for comparison.

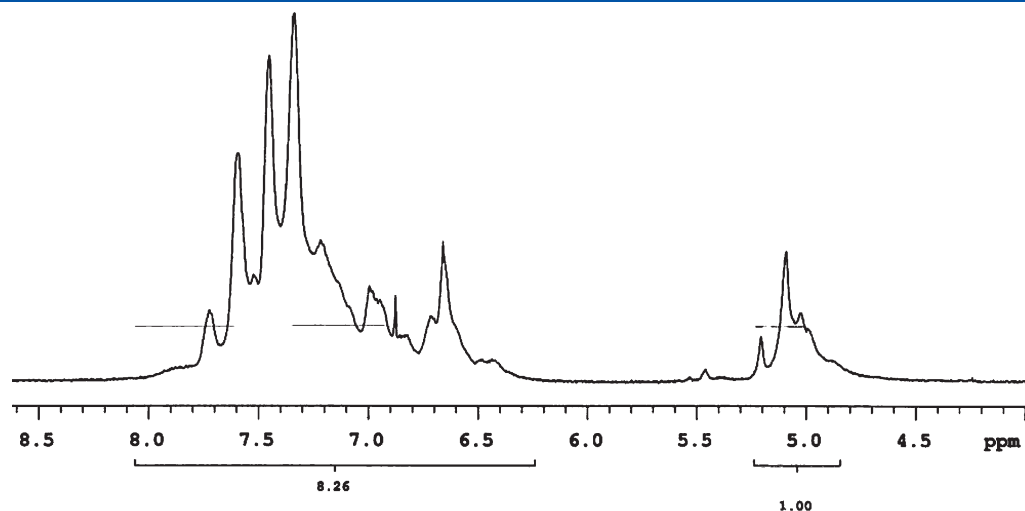


Figure 6. ¹H NMR of [(NH₂Ph)_{2x}Ph_{10/12-x}(SiO_{1.5})_{10/12}] (fraction 3) in DMSO-*d*₆.

Differential Scanning Calorimetry (DSC). Calorimetry was performed on materials using a DSC 2910 (TA Instruments, Inc., New Castle, DE). The N₂ flow rate was 60 mL/min. Samples (10–15 mg) were placed in a pan and ramped to 400 °C (5 °C/min/N₂) without capping.

RESULTS AND DISCUSSION

On the basis of our experience with the Scheme 3 vinyl/phenyl SQ equilibration studies, we began with efforts to identify an OPS:OAPS ratio that would provide statistically controllable mixtures of cages, as seen in Scheme 4. Note that for the purposes of visual simplification we have redrawn the T₁₀ and T₁₂ structures as shown above.

In the following sections, we first discuss the synthesis of mixtures of di- and trifunctional T₁₀ and T₁₂ aminophenyl SQs and their characterization. We then describe their reactions with the diglycidyl ether of bisphenol A (DGEBA) and the characterization of the resulting polymer. We present here studies designed to provide a basic aromatic amine model for BoC syntheses of related epoxy resins systems and for future amidation and imidation studies.

Synthesis of [(NH₂Ph)_{2x}Ph_{8/10-x}(SiO_{1.5})_{10/12}]. On the basis of our first two studies,^{28,29} we explored the catalytic rearrangement of OPS/OAPS mixtures with TBAF targeting di- and triamino SQs per Scheme 4. Figure 1 and Table 1 provide MALDI ToF data for a 3:1 mole ratio following 72 h of reaction. The Figure 1 spectrum shows a mixture of the T₈, T₁₀, and T₁₂ cages (major product is T₁₀) with aminophenyl group contents ranging from 0 to 5 but with ≈20% quantities of unsubstituted SQs.

The OPS:OAPS ratios were varied to optimize diaminophenyl contents, per Table 2. In the case of the 4:1 OPS:OAPS reaction, the main products are monoaminophenyl SQ compounds. Although the 2.5:1 of OPS:OAPS reaction shows diaminophenyl SQ compounds as the main product like the 3:1 of OPS:OAPS reaction, the relative peak intensities of triaminophenyl SQ compounds in the MALDI are higher than for 3:1 of OPS:OAPS. Given that triaminophenyl SQ compounds could form cross-link points during the polymerization that would be difficult to separate from diaminophenyl SQ compounds by column chromatography due to their very similar chemical

structures and properties (e.g. solubility), we decided to use the 3:1 of OPS:OAPS ratio as an optimum.

Because the unsubstituted SQs are relatively insoluble, we chose to recover the soluble products via column chromatography (see Experimental Section) and thereafter isolate the mono- and diamino components as a prelude to synthesizing a “linear” polymer. Because we have no way of knowing the exact placement of the amino groups on the phenyl rings (*p:m:o* ratios are 1:1:0¹⁶) and the amino group positions on the T₁₀ and T₁₂ cages are unknown, the concept of linear is not really correct but offers the simplest descriptor.

Elution using dichloromethane:hexane (8:2) gave fractions 1 (*R_f* value: 0.9) and 2 (*R_f* value: 0.6) separate from the original crude, dark brown mixture. After fraction 2 eluted, the elution solvent was changed to THF to obtain fraction 3. The MALDI-TOF of fractions 1, 2, and 3 are shown in Figures 2–4, respectively.

MALDI-TOF spectra show that fraction 1 consists of a mixture of OPS and DPS (decaphenyl SQ). Fraction 2 is mostly monoaminophenyl SQ (T₁₀), whereas fraction 3 is a mixture of the desired diaminophenyl SQs (T₁₀ and T₁₂) and triaminophenyl SQ (T₈). It is important to note that MALDI intensity data often do not provide a direct quantification of the species present as the intensities relate to the facility with which the individual components ionize. Thus, these data are best considered as being qualitatively similar to the actual isomer compositions.

The TGAs of fraction 3, OPS, and OAPS in air are shown in Figure 5. The TGA of fraction 3 reveals high thermal stability (*T_{d5%}* = 450 °C) and a ceramic yield to SiO₂ of 45.2% (Table 6). The ceramic yield indicates that the ratio of aminophenyl to phenyl groups is 27:73. This ratio can be used to calculate an 8.8:1 phenyl:amine proton ratio matching the 8.3:1 integration of Figure 6.

Figure 7 provides GPC data (THF) for the starting compounds, the crude reaction mixture and Fraction 3. Table 5 provides relevant molecular weights and polydispersities for the same materials. The molecular weights are measured against

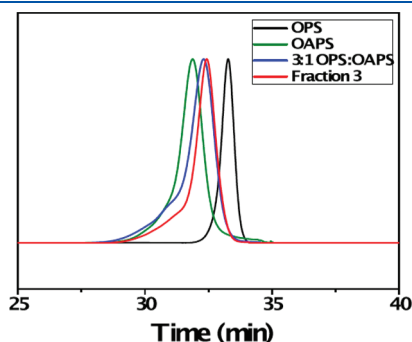


Figure 7. GPC (THF) of the starting compounds, the crude reaction mixture, and fraction 3.

polystyrene standards and are always lower than the estimated values because of the spherical nature of the SQs.

Polymerization of [(NH₂Ph)_{2x}Ph_{8/10-x}(SiO_{1.5})_{10/12}] and DGEBA. Fraction 3, consisting primarily of [(NH₂Ph)_{2x}Ph_{8/10-x}(SiO_{1.5})_{10/12}], was reacted with DGEBA in effort to form a BoC polymer per Scheme 5. Again for the purposes of visual simplification, we have simplified the mixed cages as spheres/beads to imply a BoC type of oligomer.

In this polymerization, when DGEBA was added at 1:1 mole ratio of [epoxy]:[amine], insoluble cross-linked polymer was observed to form as might be expected given that fraction 3 includes triamino-functionalized cages. Therefore, the amount of DGEBA and reaction time were adjusted to eliminate formation of insoluble material. By trial and error, we found that a 0.8:1 ratio of [epoxy]:[amine] provided a soluble high molecular weight polymer. Thus, Figure 8 provides GPC traces following the polymerization process with time at this stoichiometry. Initially, only low MW oligomers are observed until the last 3 h of reaction.

At 24 h of reaction time, the synthesized BoC polymers are soluble in THF and exhibit a bimodal molecular weight distribution

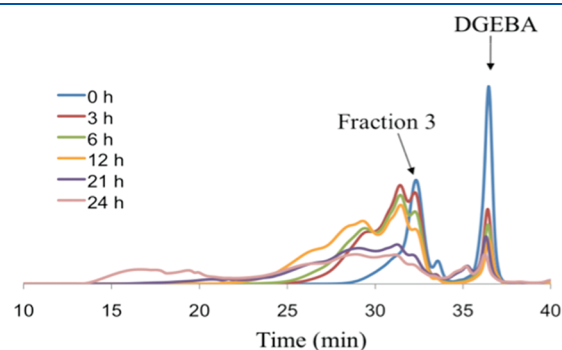


Figure 8. Progress of fraction 3 and DGEBA polymerization, monitored by GPC.

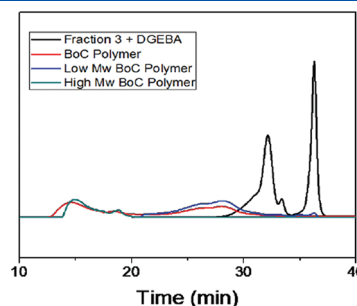
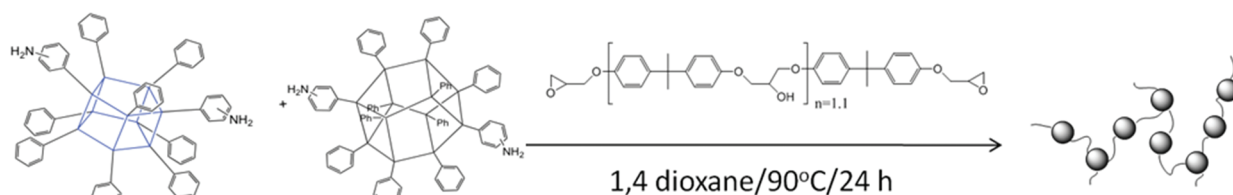


Figure 9. GPC trace of fraction 3 and DGEBA mixture, BoC polymer after 24 h, separated low and high molecular weight BoC polymers.

Scheme 5. BoC Polymerization of [(NH₂Ph)_{2x}Ph_{10/12-x}(SiO_{1.5})_{10/12}] with DGEBA



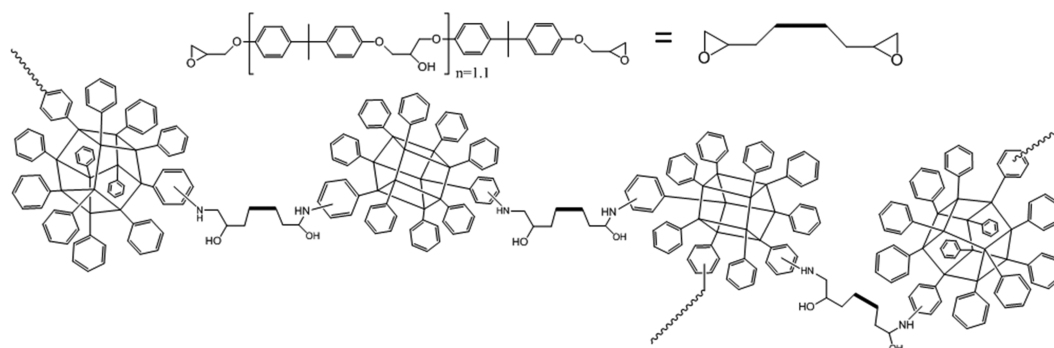


Figure 10. General epoxy coupling reaction.

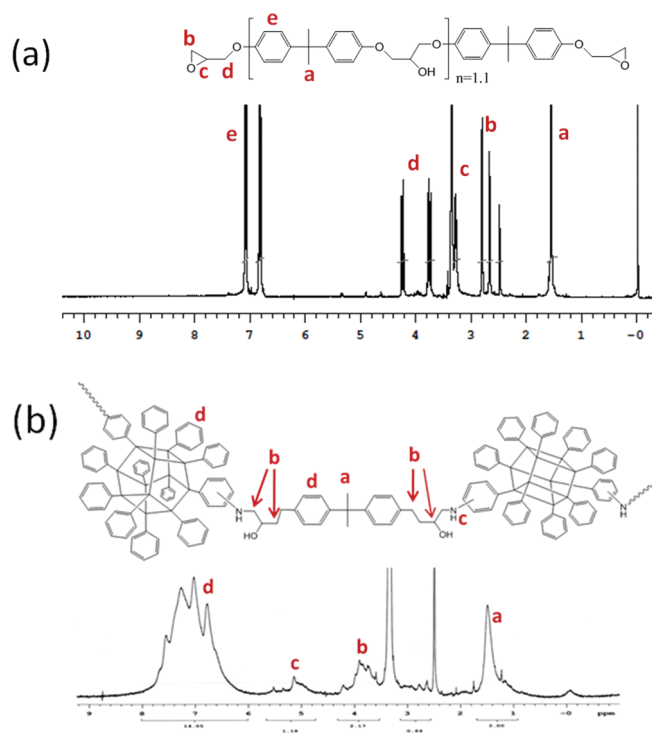


Figure 11. ^1H NMR for (a) DGEBA and (b) BoC polymer in $\text{DMSO}-d_6$.

by GPC as seen in Figures 8 and 9. The bimodal components can be purified by precipitation using solubility differences. The low MW polymers dissolve easily in THF on stirring for 2 h at ambient. In contrast, the high molecular weight polymers must be sonicated to dissolve. Figure 9 records the GPC traces for the mixture of fraction 3 and DGEBA, the as-formed BoC polymer, and its fractional dissolution products (see Experimental Section).

As pointed out by a referee, some DGEBA remains after 24 h of reaction despite a starting stoichiometry that should have all the DGEBA consumed. The explanation for this as well as the formation of a bimodal distribution can be explained in several ways. First, it is important to note that although fraction 3 consists of both di- and triamino- cages, the exact position of amino groups on the “spherical” surface of the cages is unknown. It is possible that some of these groups are adjacent to each other. Thus, one could envision that epoxy reactions will lead to compounds wherein it is possible to form cyclomers. If the average MW of the monomer unit is of the order of 1700–1900 Da, then one can envision a cyclic with three repeat units in it.

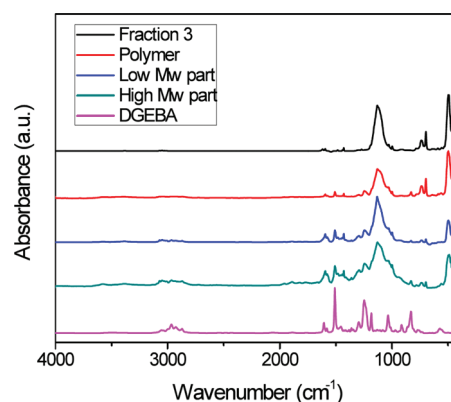


Figure 12. IR spectra of monomers and synthesized polymers for comparison.

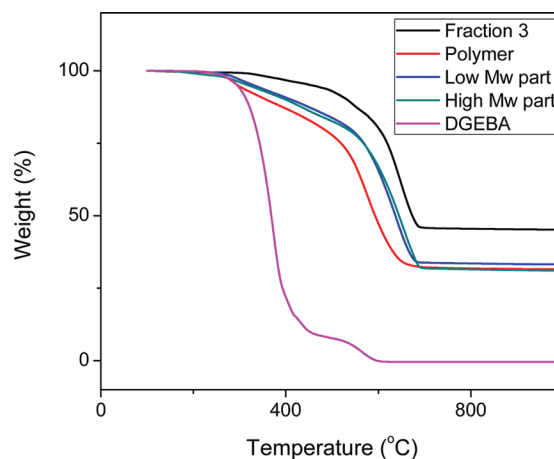


Figure 13. TGA of the synthesized polymer and starting materials for comparison in air ($10\text{ }^\circ\text{C}/\text{min}$).

Alternately, the epoxy reaction of Figure 10 will first produce “linear” oligomers where some of the cages will have a third NH_2 — group. One can envision that after two epoxy linkages form this third NH_2 — may be sufficiently sterically encumbered as to be much less reactive. At some point, as amine functionalities react, those left will be these encumbered sites. Thus, despite the initial stoichiometry, some DGEBA molecules might not be able to access these sites, leading to the observation of residual DGEBA despite the initial stoichiometry.

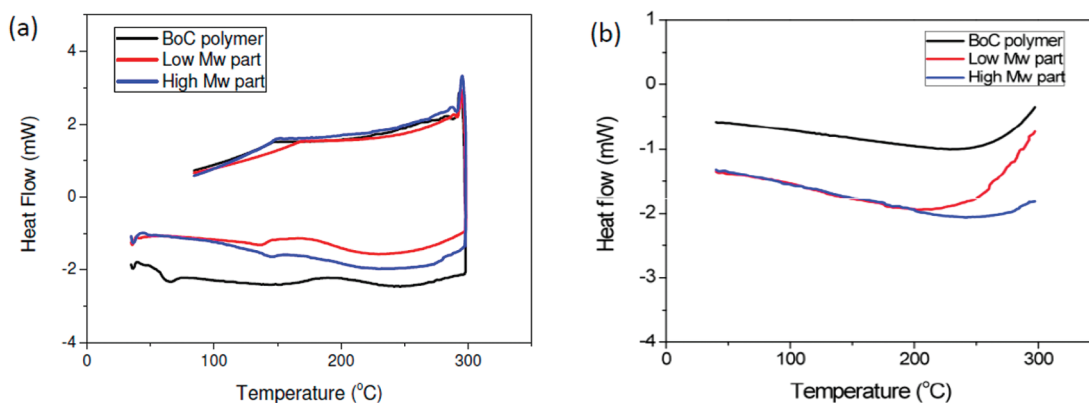


Figure 14. (a) First and (b) second DSC of BoC polymer, high M_w part, and low M_w part.

Eventually, they may react. This process will produce branches and or cross-links between shorter chains leading to very non-linear but higher MW species and/or species with several links between shorter chains. One might then suggest that the “interior” of these species will be less accessible to solvent, resulting in quite different behavior to a common solvent. This seems most likely given the propensity to form insoluble materials at a 1:1 mole ratio of epoxy to amine as used traditionally.

While all species are soluble in the original reaction solution at 90 °C, on precipitation only the low MW species are readily soluble in cold THF. The higher MW polymer only dissolved when heated to ≈ 60 °C but dissolve readily using ultrasonication. These aspects suggest difficult in solvating “interior” components, supporting the above speculation. Indeed, it is possible to suggest that the “interior” species react to form internal cyclics that will not solvate easily leading to the observed differences in solubility. This seems to be a better explanation than “lightly cross-linked”.

A further point made by a referee that we agree with is the fact that we have used polystyrene standards where the highest MW 900 000 Da. Consequently, the Table 8 data must be viewed at best as qualitative since we are reporting values well outside those we are actually calibrated to assess.

NMR Studies. In efforts to understand the structure of the BoC products, we briefly explored ^1H NMR characterization. Thus, Figure 11 provides the NMR of BoC polymer, the starting DGEBA oligomer. The integration ratio of amino to phenyl proton of fraction 3 and BoC polymer changes from 1:10.8 to 1:11.9. Also, the alkyl proton (Ha, Hd) peaks broadened, as might be expected, after polymerization. These mean the DGEBAs are incorporated in the BoC polymers.

FTIR Studies. Complementary IR studies are presented in Figure 12. In general, the FTIR of the high MW and low MW fractions are quite similar except for a slight broadening in the high MW materials at 1050 cm^{-1} in a region attributable to $\nu\text{C}-\text{O}$. Otherwise, the FTIRs are as expected for these compounds based on our previous work.³¹

Figure 13 shows TGAs of BoC polymer and starting materials. Table 9 shows $T_{\text{d}5\%}$ for the high and low MW polymers to be 320–330 °C in air as expected from previously published studies on OAP/DEGEB nanocomposites.³¹ The ceramic yields for both systems are $32 \pm 1\%$. The lower ceramic yield found for the BoC polymer compared to fraction 3 arises because the polymer incorporates DGEBA which dilutes the total silica mass.

DSC studies shown in Figure 14 suggest an initial T_g for both the low and high MW components at ≈ 125 °C which disappears in the second cycle likely as a result of extended cross-linking that occurs as DGEBA units that are singly reacted within the polymer chain find free NH_2 groups to react with or that undergo ring-opening self-polymerization. After the second cycle, the resulting resin is no longer THF soluble, supporting the idea that cross-linking has occurred.

CONCLUSIONS

We find that it is quite possible to develop routes to BoC epoxy resin systems that are soluble and processable if one is careful to control the amine:epoxy ratios. A related paper to be submitted shortly provides a parallel approach wherein an alkyl amine group is used in place of an aromatic amine, extending the generality of this approach. In future papers, we plan to present mechanical properties data as shown in the accompanying paper and also to extend the current studies to amides and imides. Finally it is important to recognize that the insolubles from this system may be redissolved by addition of more OPS and a catalytic amount of F^- making these systems recyclable.

ACKNOWLEDGMENT

We thank DOE for support of the synthesis part of this work through DOE Center Grant Award No. DE-SC0000957 and Boeing Inc. for support of the characterization work. We also thank a referee for very careful reading of the manuscript and also quite helpful comments.

REFERENCES

- (1) Voronkov, M. G.; Lavrent'yev, V. I. Polyhedral Oligosilsesquioxanes and Their Homo Derivatives. *Top. Curr. Chem.* **1982**, *102*, 199–236.
- (2) Baney, R. H.; Itoh, M.; Sakakibara, A.; Suzuki, T. *Silsesquioxanes*. *Chem. Rev.* **1995**, *95*, 1409–30.
- (3) Loy, D. A.; Shea, K. J. Bridged Polysilsesquioxanes. Highly Porous Hybrid Organic-Inorganic Materials. *Chem. Rev.* **1995**, *95*, 1431–42.
- (4) Calzaferri, G. Silsesquioxanes. In *Tailor-made Silicon-Oxygen Compounds, from molecules to materials*; Corriu, R., Jutzi, P., Eds.; Publ. Friedr. Vieweg & Sohn mbH: Braunschweig/Weisbaden, Germany, 1996; pp 149–169.
- (5) Lichtenhan, J. Silsesquioxane-based Polymers. In *Polymeric Materials Encyclopedia*; Salmone, J. C., Ed.; CRC Press: New York, 1996; Vol. 10, pp 7768–77.

- (6) Provatas, A.; Matison, J. G. Synthesis and applications of silsesquioxanes. *Trends Polym. Sci.* **1997**, *5*, 327–33.
- (7) Li, G.; Wang, L.; Ni, H.; Pittman, C. U. Polyhedral Oligomeric Silsesquioxane (POSS) Polymers and Copolymers: A Review. *J. Inorg. Organomet. Polym.* **2001**, *11*, 123–151.
- (8) Duchateau, R. Incompletely Condensed Silsesquioxanes: Versatile Tools in Developing Silica-Supported Olefin Polymerization Catalysts. *Chem. Rev.* **2002**, *102*, 3525–3542.
- (9) Abe, Y.; Gunji, T. Oligo- and polysiloxanes. *Prog. Polym. Sci.* **2004**, *29*, 149–182.
- (10) Phillips, S. H.; Haddad, T. S.; Tomczak, S. J. Developments in Nanoscience: polyhedral oligomeric silsesquioxane (POSS)-polymers. *Curr. Opin. Solid State Mater. Sci.* **2004**, *8*, 21–29.
- (11) Laine, R. M. Nano-building blocks based on the $[\text{OSiO}_{1.5}]_8$ silsesquioxanes. *J. Mater. Chem.* **2005**, *15*, 3725–44.
- (12) Lickiss, P. D.; Rataboul, F. Fully Condensed Polyhedral Silsesquioxanes: From Synthesis to Application. *Adv. Organomet. Chem.* **2008**, *57*, 1–116.
- (13) Chan, K. L.; Sonar, P.; Sellinger, A. Cubic silsesquioxanes for use in solution processable organic light emitting diodes (OLED). *J. Mater. Chem.* **2009**, *19*, 1–19.
- (14) Kannan, R. Y.; Salacinski, H. J.; Butler, P. E.; Seifalian, A. M. Polyhedral Oligomeric Silsesquioxane Nanocomposites: The Next Generation Material for Biomedical Applications. *Acc. Chem. Res.* **2005**, *38*, 879–884.
- (15) Cordes, D. B.; Lickiss, P. D.; Franck, R. Recent Developments in the Chemistry of Cubic Polyhedral Oligosilsesquioxanes. *Chem. Rev.* **2010**, *10*, 2081–2173.
- (16) Laine, R. M.; Roll, M. F. Polyhedral Phenylsilsesquioxanes. *Macromolecules* **2011**, *44*, 1073–1220.
- (17) Wu, J.; Mather, P. T. POSS Polymers: Physical Properties and Biomaterials Applications. *Polym. Rev.* **2009**, 25–63.
- (18) Li, Z.; Kawakami, Y. Formation of Incompletely Condensed Oligosilsesquioxanes by Hydrolysis of Completely Condensed POSS via Reshuffling. *Chem. Lett.* **2008**, *37*, 804–05.
- (19) Morimoto, Y.; Watanabe, K.; Ootake, N.; Inagaki, J.; Yoshida, K.; Ohguma, K. Silsesquioxane Derivatives and Process or Production Therefor. U.S. Patent Application 20040249103A1, Sept 2002.
- (20) Seino, M.; Hayakawa, T.; Ishida, Y.; Kakimoto, M.; Watanabe, K.; Oikawa, H. Hydrosilylation Polymerization of Double-Decker-Shaped Silsesquioxane Having Hydrosilane with Diynes. *Macromolecules* **2006**, *39*, 3473–3475.
- (21) Yoshida, K.; Hattori, T.; Ootake, N.; Tanaka, R.; Matsumoto, H. Silsesquioxane-Based Polymers: Synthesis of Phenylsilsesquioxanes with Double-Decker Structure and Their Polymers. In *Silicon Based Polymers*; Ganachaud, F., Boileau, S., Boury, B., Eds.; Springer: Dordrecht, 2008; pp 205–211.
- (22) Hoque, Md. A.; Kakihana, Y.; Shinke, S.; Kawakami, Y. Polysiloxanes with Periodically Distributed Isomeric Double-Decker Silsesquioxane in the Main Chain. *Macromolecules* **2009**, *42*, 3309–3315.
- (23) Wu, S.; Hayakawa, T.; Kikuchi, R.; Grunzinger, S. J.; Kakimoto, M.; Oikawa, H. Synthesis and Characterization of Semiaromatic Polyimides Containing POSS in Main Chain Derived from Double-Decker-Shaped Silsesquioxane. *Macromolecules* **2007**, *40*, 5698–5705.
- (24) Lichtenhan, J. D.; Vu, N. Q.; Carter, J. A.; Gilman, J. W.; Feher, F. J. Silsesquioxane-siloxane copolymers from polyhedral silsesquioxanes. *Macromolecules* **1993**, *26*, 2141–2142.
- (25) Takahashi, K.; Sulaiman, S.; Katzenstein, J. M.; Snoblen, S.; Laine, R. M. New Aminophenylsilsesquioxanes, Synthesis, Properties and Epoxy Nanocomposites. *Aust. J. Chem.* **2006**, *59*, 564–70.
- (26) Roll, M. R.; Takahashi, K.; Mathur, P.; Kampf, J. W.; Laine, R. M. $[\text{PhSiO}_{1.5}]_8$ autocatalytically brominates to produce $[\text{o-BrPhSiO}_{1.5}]_8$. Further bromination gives crystalline $[\text{2,5-Br}_2\text{PhSiO}_{1.5}]_8$ with a density of 2.38 g/cm^3 and calculated refractive index of 1.7 (RI of sapphire is 1.76) or the tetracosabromo compound $[\text{Br}_3\text{PhSiO}_{1.5}]_8$. Submitted for publication.
- (27) Sulaiman, S.; Zhang, J.; Goodson, T., III; Laine, R. M. Synthesis, Characterization and Photophysical Properties of Polyfunctional Phenylsilsesquioxanes: $[\text{o-RPhSiO}_{1.5}]_8$, $[\text{2,5-R}_2\text{PhSiO}_{1.5}]_8$, and $[\text{R}_3\text{PhSiO}_{1.5}]_8$. Submitted for publication.
- (28) Asuncion, M. Z.; Laine, R. M. Fluoride Rearrangement Reactions of Polyphenyl- and Polyvinylsilsesquioxanes as a Facile Route to Mixed Functional Phenyl/Vinyl T_{10} and T_{12} Silsesquioxanes. *J. Am. Chem. Soc.* **2010**, *132*, 3723–3736.
- (29) Ronchi, M.; Sulaiman, S.; Boston, N. R.; Laine, R. M. Fluoride catalyzed rearrangements of polysilsesquioxanes, mixed Me, vinyl T_8 , Me, vinyl T_{10} and T_{12} cages. *Appl. Organomet. Chem.* **2009**, *24*, 551–557.
- (30) Samthong, C.; Laine, R. M.; Somwangthanaroj, A. Synthesis and characterization of organic/inorganic epoxy composites from poly-(aminopropyl/phenyl)silsesquioxanes. To be submitted.
- (31) Tamaki, R.; Tanaka, Y.; Asuncion, M. Z.; Choi, J.; Laine, R. M. Octa(aminophenyl)silsesquioxane as a Nanoconstruction Site. *J. Am. Chem. Soc.* **2001**, *123*, 12416–7.